https://doi.org/10.5194/nhess-2024-217
Preprint. Discussion started: 15 January 2025

Natural Hazards and Earth System Sciences
Discussions

Improving Forest Damage Detection and Risk Assessment from Winter Storms Using High-Resolution Satellite Data and Environmental Drivers

Kirill Korznikov[1,2], Dmitriy Kislov[2], Jiří Doležal[1], Jan Altman[1,3]

[1]Institute of Botany of the CAS, 379 01 Třeboň, Czech Republic
[2]Botanical Garden-Institute FEB RAS, 690024 Vladivostok, Russia
[3]Faculty of Forestry and Wood Sciences, Czech University of Life Sciences Prague, 165 21 Prague, Czech Republic

Correspondence to: Kirill Korznikov (korzkir@gmail.com)

Abstract. Accurate assessment of forest losses and evaluation of future damage risks are crucial for effective forest management and conservation, particularly as global warming intensifies natural disturbance agents. This study introduces a novel approach combining convolutional neural networks (CNNs) with Random Forest (RF) machine learning classifiers to enhance the precision of forest disturbance detection and risk evaluation. We tested this approach on a large-scale dataset (1490 km2) with diverse forest types and environmental conditions of cool temperate-south boreal forests on Kunashir Island (Northwest Pacific). Using the U-Net deep learning architecture, we precisely identified windthrow patches from (VHR) Pléiades-1 optical satellite imagery. Resulted windthrow map was integrated with an RF classifier that utilized environmental predictors, including elevation, slope aspect, slope inclination, slope curvature, forest canopy closure, landform type, and forest vegetation type, to assess forest damage risk. Our analysis revealed approximately 21.73 km^2 of the forested area as significantly disturbed, predominantly within dark coniferous forests. Elevation emerged as the most critical predictor of disturbance risk, with complex interactions observed among predictors such as canopy closure and slope steepness. This integrated approach allowed for highly accurate forest loss detection and provided valuable insights into the risk of future damage events. By combining advanced deep learning techniques with RF and detailed environmental predictors, this approach offers a robust framework for evaluating forest disturbance risk. This method pushes forward the frontiers in the precision of forest loss detection but also aids in developing effective strategies for managing and mitigating risks from future disturbance events.

1 Introduction

Modern remote sensing techniques enable the detection of disturbed forest areas across diverse forest ecosystems (Curtis et al., 2018; Hansen et al., 2013; Tyukavina et al., 2022). Accurate mapping of disturbances and their correlation with potential risk factors enhances the precision of windthrow risk assessments (Suvanto et al., 2019). This approach provides a deeper understanding of how various disturbance events, such as storms, tropical and extratropical cyclones (TCs and ETCs), or

https://doi.org/10.5194/nhess-2024-217
Preprint. Discussion started: 15 January 2025


Natural Hazards and Earth System Sciences Discussions

tornadoes impact forest ecosystems. Ultimately, it allows for the refinement of forest disturbance risk assessments and the integration of these considerations into forestry planning efforts.

Until recently, a limitation existed in the spatial resolution of freely available satellite images. The Moderate Resolution Imaging Spectroradiometer (MODIS) had a resolution of 250 m pixel-1, only allowing for identifying extensive forest canopy disturbances (Jin and Sader, 2005). The modern Landsat-8 satellite offers a resolution of 30 m pixel-1 (Hansen et al., 2013), and the Sentinel-2 mission provides a maximal resolution of 10 m pixel-1 (Zhang et al., 2021). Such resolutions enable the reliable identification of even intermediate-size patches of disturbed forests but may not be sufficient to detect small canopy gaps (Chen et al., 2021). The development of remote sensing methods and the advancement of open data policies have substantially increased the quantity, quality, and availability of high-resolution data (<1 m pixel-1). This progress opens new possibilities for the detailed spatial estimation of forest sensitivity to disturbances. Very high-resolution (VHR) satellite optical data and advanced convolutional machine learning techniques, such as semantic segmentation neural networks, enable the delineation of disturbed areas down to small canopy gaps (Kattenborn et al., 2021; Kislov et al., 2021). The advancements in machine learning and the availability of satellite images have unlocked the potential for precise analysis of the linkage between forest disturbances caused by atmospheric events and environmental predictors, such as terrain features (Korznikov et al., 2022).

Global climate changes are escalating the risks associated with natural forest disturbances, including cyclonic vortices of both tropical and extratropical origins (Little et al., 2023; Priestley and Catto, 2022). A convergence of extreme wind speeds and heavy precipitation leads to significant economic losses (Montagné-Huck and Brunette, 2018; Sánchez et al., 2021; Roos, 2023). Beyond direct damage, these substantial disturbances can trigger a cascade of ecological consequences, potentially exacerbating, or even surpassing, the impact of an initial disturbance (Seidl et al., 2017; Seidl and Rammer, 2017). Large-scale forest disturbances significantly affect the carbon cycle, influencing carbon turnover times, climate regulation services, and the social costs associated with carbon emissions (Anderson-Teixeira et al., 2021; Liu et al., 2011; Pugh et al., 2019). Therefore, evaluating the impact of various disturbance agents on different forest types is crucial for assessing future risks to forest ecosystems (Altman et al., 2024).

Wind is the primary factor responsible for cyclone disturbances, directly causing mechanical stress that leads to tree falls and breakage (Everham and Brokaw, 1996; Foster, 1988). The severity of windthrow is influenced by numerous factors, such as terrain conditions, forest canopy closure, and vegetation type, which can either increase or decrease a forest's vulnerability to windthrow (Mitchell, 2013). Consequently, assessing the risk of forest cyclone disturbances is an essential task in forest and environmental management (Seidl and Turner, 2022; Thom and Seidl, 2016).

To test the new approaches for disturbance detection, it is necessary to have a diverse study area (from geomorphological and forest types of perspective and cloudless VHR satellite images. Our study assesses forest damage caused by a severe winter extratropical cyclone (ETC) using VHR satellite images from the Pléiades-2 satellite (50 cm pixel-1). For this purpose, we employ the U-Net semantic segmentation convolutional neural network (CNN) to detect forest damage and use the Random Forest (RF) algorithm to evaluate vulnerability risk, incorporating geomorphological features, forest canopy closure, and forest

https://doi.org/10.5194/nhess-2024-217
Preprint. Discussion started: 15 January 2025


Natural Hazards and Earth System Sciences Discussions

types. The Kunashir Island (the Kuril Islands), with its diverse terrain and various types of pristine forests. In addition, was affected by severe ETC on December 17, 2014, bringing intense wet snow and winds exceeding 50 ms-1, resulting in extensive forest damage, including hundreds of hectares of fallen forest patches. Hence, it represents an ideal set of conditions for applying our CNN-based approach, enhancing our understanding of varying degrees of forest vulnerability and resistance to disturbances.

Snowstorms from ETCs are common in northern temperate and boreal zones (Barrere et al., 2023), and the frequency of extreme winter ETCs in the Northern Hemisphere is projected to increase by 4% by the end of the 21st century, particularly in the Northwest Pacific and the transition zone between Eurasia and the Pacific Ocean (Priestley and Catto, 2022). This underscores the need for advanced technologies in assessing forest damage and risk, addressing not only ETCs but also a broad range of abiotic and biotic damage agents. Our study highlights the importance of integrating new methodologies for evaluating forest damage and risk, thereby enhancing forest management and ecological resilience strategies in response to increasingly extreme weather events.

Specifically, our objectives are to (i) create a precise forest disturbance map using VHR imagery and the deep learning U-Net semantic segmentation CNN; (ii) calculate and compare the distribution of disturbed patches relative to the entire forest cover across environmental predictors; and (iii) determine the strongest environmental predictors of the risk of disturbance caused by ETC events. We hypothesize that a vulnerability of forest cover to ETC-induced disturbances is linked to topographic attributes, forest canopy closure, and specific forest types

2 Material and methods

2.1 Study Area

Kunashir, a volcanic island with an area of over 1,490 km², is located in the southern part of the Kuril Islands, an archipelago elongated more than 1,200 km from Japan to Kamchatka (Fig. 1). Kunashir features rugged terrain with four active volcanoes, with its highest peak reaching 1,819 meters above sea level. According to the Yuzhno-Kurilsk weather station (World Weather Organization code 32165), the average annual temperature is +5.5°C, with mean annual precipitation of 1,260 mm. Kunashir is susceptible to ETCs throughout the year which come from the south or southeast and bring a lot of precipitation and heavy gusty winds.

https://doi.org/10.5194/nhess-2024-217
Preprint. Discussion started: 15 January 2025

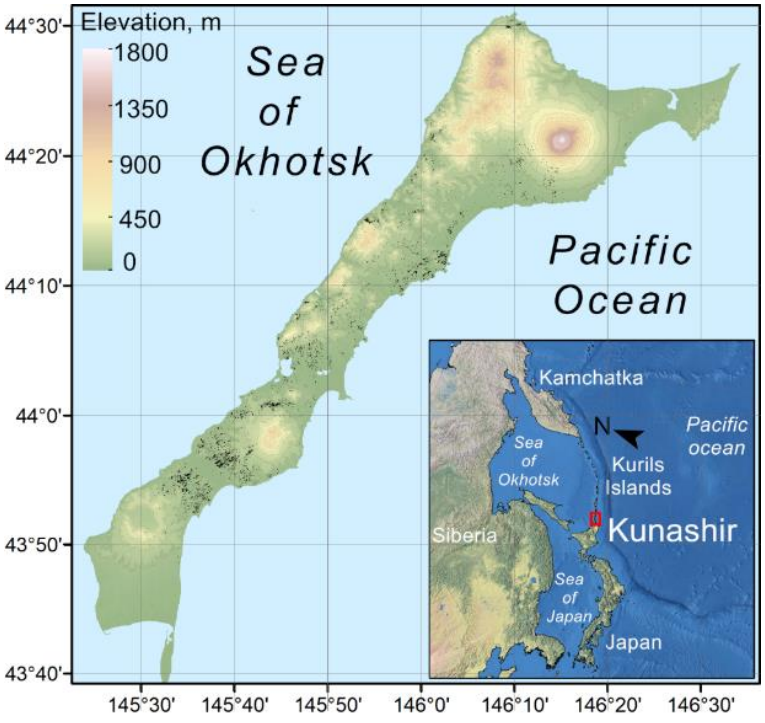

Figure 1: Geographical overview and windthrow impact on forest cover of Kunashir Island during the extratropical cyclone disturbance event. The relief map of Northeast Asia is based on data from an i-cubed eTOPO 1:250,000-scale map from the source "USA Topo Maps" (https://www.arcgis.com/home/item.html?id=99cd5fbd98934028802b4f797c4b1732).

The forest vegetation of Kunashir Island covers approximately 80% of the territory. The zonal, or climate-determinate vegetation (Pojar et al., 1987), primarily consists of southern boreal forests dominated by coniferous evergreen trees. A spruce forms forest stands in swamps and volcanic deposits. Temperate broadleaf and mixed forests, featuring a diverse mix of tree species such as maples and oaks, are located on the warmer southwestern coast of the island. Monodominant oak stands are prevalent in the southern part of the island, while boreal forests predominate in the north. Mixed boreal forests consist of fir, spruce, and stone birch (*Betula ermanii* Cham.). Stone birches also form secondary forest stands. At higher elevations, such as mountain peaks and volcanic ridges, thickets of dwarf pine dominate. Stands of alder and various willows are typical in riparian zones. In deforested areas, thickets of dwarf bamboo (*Sasa* spp.) with single or sparse trees are common (Korznikov et al. 2024). Even the limited forest management on the island ceased in the mid-20th century, and almost half of the island is now designated as a nature reserve. Consequently, the vegetation cover on Kunashir is largely representative of the natural, undisturbed forests typical of the transition zone between temperate deciduous and southern coniferous boreal forests. The vegetation map of Kunashir Island is available in Fig. 2.

https://doi.org/10.5194/nhess-2024-217
Preprint. Discussion started: 15 January 2025

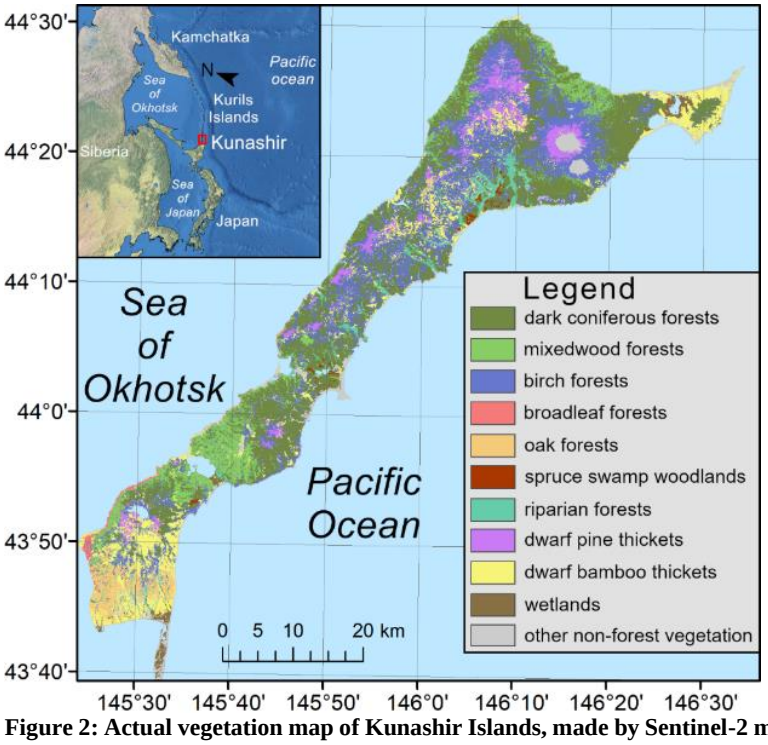

Figure 2: Actual vegetation map of Kunashir Islands, made by Sentinel-2 multispectral satellite images. The relief map of Northeast Asia is based on data from an i-cubed eTOPO 1:250,000-scale map from the source "USA Topo Maps" (https://www.arcgis.com/home/item.html?id=99cd5fbd98934028802b4f797c4b1732).

2.2 Extratropical Cyclone Disturbance Event

An atmospheric depression originated over the East China Sea on December 15th, 2014, and migrated eastward, transforming into an ETC in the Kuroshio warm current zone in the Pacific Ocean, east of Japan. This ETC maintained its northward trajectory and eventually affected the southern part of the Kuril Islands on December 17th. An extraordinarily low atmospheric pressure of 949 hPa was recorded at the ETC's center during this event. In the northern hemisphere, such low-pressure levels are typical for the centers of TCs but are less common for ETCs. Throughout the ETC event in Kunashir, air temperatures ranged from -0.1 to +2.7 °C. The total precipitation of 39 mm, primarily in the form of wet snow, resulted in an 80 mm snow cover within 24 hours. A combination of wet snow adhering to tree crowns and exceptionally strong wind gusts triggered extensive windthrows. Specifically, data from the Yuzhno-Kurilsk weather station reported wind speeds exceeding 43 m s^{-1}, with gusts reaching up to 51 m s^{-1}. These strong wind gusts are extreme for this area and are comparable to those experienced during strong TC events. The prevailing wind directions were from the east and northeast.

2.3 Forest Disturbances Recognition

Due to the monsoon climate, there are very few cloudless satellite images of this area during the summer. Fortunately, the Pléiades-1 satellite system captured VHR images of Kunashir Island in June 2015, six months after the ETC disturbance event.

https://doi.org/10.5194/nhess-2024-217
Preprint. Discussion started: 15 January 2025

Natural Hazards and Earth System Sciences
Discussions

This is the only VHR satellite image available for the entire island. VHR optical images (0.5 m pixel^{-1}) were utilized to precisely identify disturbances using the semantic segmentation U-Net CNN (Kislov et al., 2021; Kislov and Korznikov, 2020). The achieved level of accuracy was 0.92, as determined by the balanced accuracy (BA) and F1 metrics, and the Intersection over the Union metric. Following recognition, we excluded polygons representing small canopy gaps smaller than 10 m², corresponding to single broken trees, using the software ArcMap 10.8.2. An example of the recognition result on a VHR satellite image is presented in Fig. 3. The Python code for training and applying the U-Net CNN is provided in Supplementary 1.

Figure 3: Results of windthrow detection utilizing the U-Net neural network. The satellite image was taken by the Pléiades-1.

2.4 Environmental Predictors

To identify the environmental factors influencing forest damage risk, we compiled a set of 7 predictors (Table 1). Elevation above sea level was derived directly from the raster data of the Advanced Spaceborne Thermal Emission and Reflection Radiometer digital elevation model (ASTER DEM) version 3, with a resolution of 30 m pixel^{-1} and vertical accuracy of 7 meters (Abrams et al., 2020). We calculated values for slope aspect (slope exposition), slope steepness, and general slope curvature using the ASTER DEM raster and the raster surface tools in the ArcMap 10.8.2 program (2024). To clarify, standard curvature values are interpreted as follows: positive values indicate an upwardly convex surface; negative values indicate an upwardly concave surface; and a value of 0 indicates a flat surface. Expected values for a hilly area (moderate relief) range

https://doi.org/10.5194/nhess-2024-217
Preprint. Discussion started: 15 January 2025

Natural Hazards and Earth System Sciences
Discussions

from −0.5 to 0.5, while for steep, rugged mountains (extreme relief), values can range between −4 and 4 (visualization in Fig. S4). Separate raster layers with a resolution of 30 m pixel^{-1} were created for each topographical predictor.

Table 1: Environmental predictors for windthrow risk assessment

Predictor	Range	Step	Data source	Type
Aspect (direction), °	0–360	10	ASTER DEM	Quantitative
Curvature	-4–4	0.5	ASTER DEM	Quantitative
Elevation, m	0–1570	10	ASTER DEM	Quantitative
Slope steepness, °	0–70	2	ASTER DEM	Quantitative
Canopy (forest closure), %	20–100	2	Global Tree Cover	Quantitative
Forest type	1, 2, …, 7	1	Vegetation map	Categorical
Landform class	1, 2, …, 10	1	ASTER DEM	Categorical

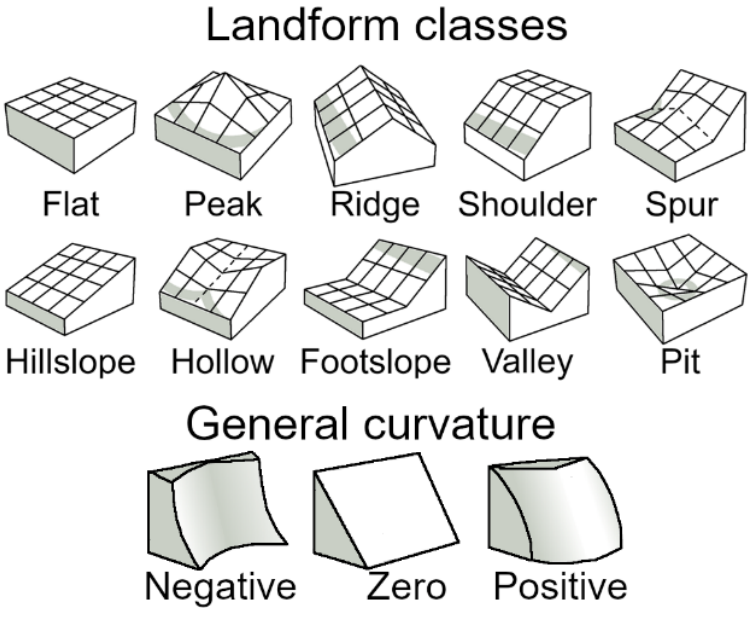

Figure 4: Visual guide to landform classification and surface curvature interpretation.

Landform types were classified using ASTER DEM data based on the system proposed by (Jasiewicz and Stepinski, 2013), containing 10 classes: 1 – peak, 2 – ridge, 3 – shoulder, 4 – spur, 5 – hillslope, 6 – footslope, 7 – flat, 8 – hollow, 9 – valley, 10 – peat (visualization in Fig. 4). We created a raster attribute of landform classes using the R toolkit r.geomorphon (available on https://github.com/OSGeo/grass/tree/main/raster/r.geomorphon), configuring the geomorph() function with a flatness threshold set at 1°, and both width and height values of the focal window set to 50 m, resulting in a raster layer with a resolution of 30 m pixel^{-1}.

https://doi.org/10.5194/nhess-2024-217
Preprint. Discussion started: 15 January 2025

Natural Hazards and Earth System Sciences
Discussions

Forest canopy closure data for the study area were sampled from the Global Tree Cover dataset (Hansen et al., 2013) with a resolution of 30 m pixel^{-1}. A canopy closure of 20% was selected as the minimal limit for forest vegetation.

The vegetation map of Kunashir Island, with a resolution of 20 meters pixel-1, was generated using multispectral Sentinel-2 satellite images, based on an original dataset of field observations and vegetation data (Korznikov et al., 2024). The classification algorithm was implemented through the multistep RF analysis. The map encompasses ten classes of vegetation units, six belonging to forest vegetation: 1 – dark coniferous (spruce and fir), 2 – mixedwood (spruce, fir, and broadleaf trees), 3 – birch, 4 – broadleaf temperate (oaks, maples), 5 – Mongolian oak, 6 – spruce swamps, 7 – riparian forests (alders and willows). The forest type was used as one of the predictors in our analysis.

Values for each environmental predictor were extracted from randomly selected points (n=20,000, with a discretization of 30 m) within windthrow patches identified by U-Net CNN (matrix #1). The same procedure was applied to 1,000,000 randomly selected points across the entire forest cover, including windthrow patches (matrix #2) and excluding windthrow patches (matrix #3). We repeated random selection for matrices #1 and #3 100 times to plot the distribution of disturbed patches and entire forest cover across the separate environmental predictors. To compare the distribution of predictors across disturbed and undisturbed patches we calculated the mean values and 95% confidence intervals. Matrix #2 was used for the RF analysis.

Some of the quantitative environmental predictors used in our analyses exhibited intercorrelation. Categorical predictors, such as landform classes and forest vegetation types, are integral characteristics connected to other predictors. For example, the upper parts of mountains are typically occupied by stone birch forests, which often feature a more open forest canopy. Different forest types also tend to occupy distinct landform classes (Fig. 5).

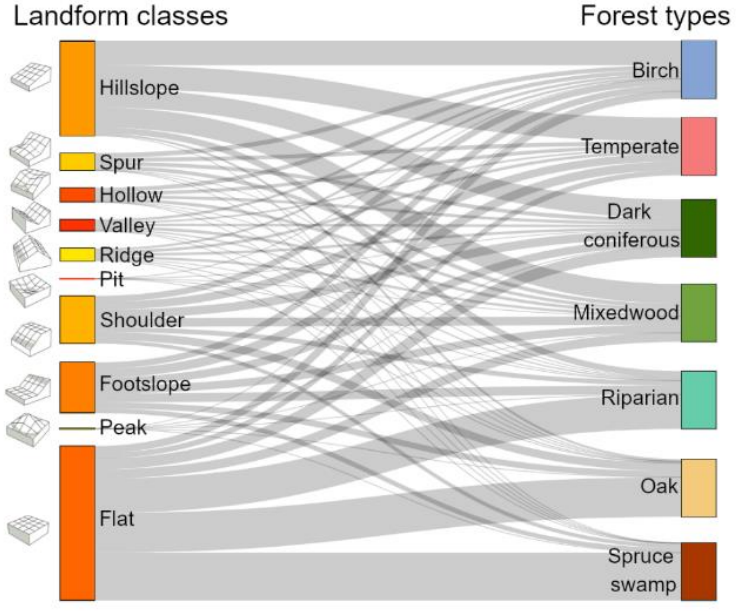

Figure 5: Proportional distribution of forest types among landform classes.

https://doi.org/10.5194/nhess-2024-217
Preprint. Discussion started: 15 January 2025

Natural Hazards and Earth System Sciences
Discussions

Therefore, using predictors separately, without considering the entire landscape context and their intercorrelations, can lead to incorrect conclusions. Matrix #3 was also used to calculate correlations between quantitative predictors using Spearman's tests in the R function cor.test() (Table 2).

Table 2: Spearman's rank correlation coefficients between quantitative predictors, the categorial predictors not included

	Aspect	Canopy	Curvature	Elevation	Slope
Aspect	1				
Canopy	-0.096	1			
Curvature	0.08	0.121	1		
Elevation	-0.025	-0.787*	0.165	1	
Slope	0.034	-0.846*	0.129	0.552*	1

*Asterisks indicate the p-value <0.05

2.4 Environmental Predictors

To discern the contribution of individual variables to the windthrow patches we employed the RF analysis from the Scikit-learn package in Python (Pedregosa et al., 2011). We conducted a grid search to identify the optimal set of hyperparameters for the RF classifier. During the grid search, 80% of the data was allocated for training and the remaining 20% for validation. The grid search yielded the following set of hyperparameters: n_estimators = 200, max_depth = 20, min_samples_split = 4,000, class_weight = 'balanced_subsample', with other parameters set to default values.

The RF classifier was trained to classify pixels as belonging to or not belonging to the windthrow patch. Given that we had six predictors (Table 1), we tested all possible combinations during the predictor selection process. Feature importance scores were calculated during both the training and validation phases. We selected the BA accuracy (BA) score metric to estimate the quality of the classification. The BA was calculated using the following equation (1):

$$\mathrm{BA} = \frac{true\ positives/(true\ positives + false\ negatives)}{true\ negatives/(true\ negatives + false\ positives)}$$

The entire methodology scheme is illustrated in Fig. 6. The Python code is available in Supplementary 2.

https://doi.org/10.5194/nhess-2024-217
Preprint. Discussion started: 15 January 2025

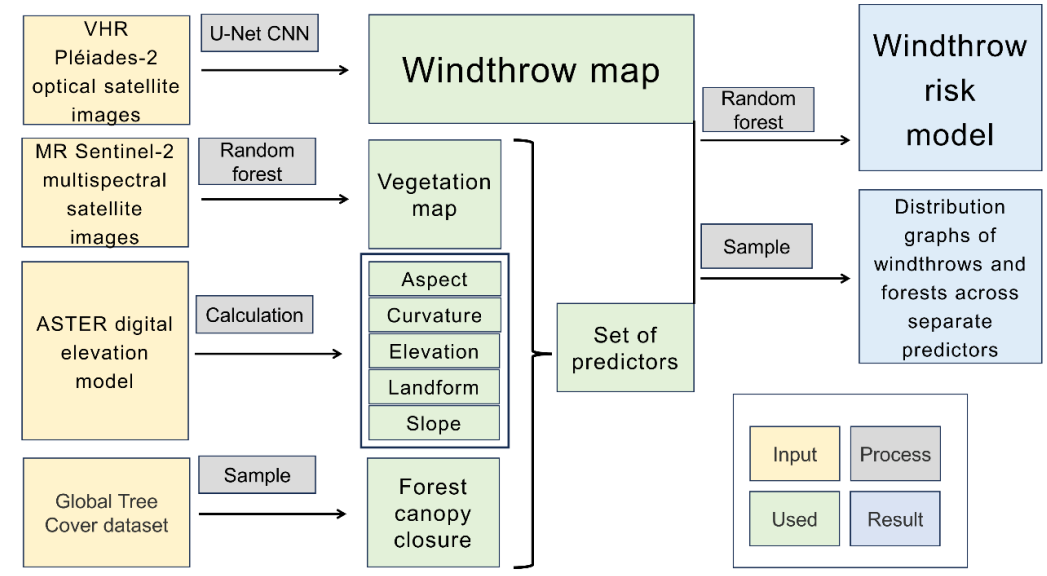

Figure 6: Workflow diagram for forest disturbance risk model development. The process begins with data input, including VHR Pléiades-1 optical satellite images and MR Sentinel-2 multispectral satellite images, both feeding into their respective analysis pathways. The U-Net CNN processes the VHR images to create a windthrow map, while the MR images contribute to the vegetation map via the RF classification. Concurrently, data from the ASTER DEM and the Global Tree Cover dataset provide topographical information and forest canopy closure, respectively, which are calculated and sampled to form a comprehensive set of predictors. These predictors then converge with the maps created from satellite images to form a complete dataset, which the RF algorithm uses to develop the windthrow risk model. Abbreviations: VHR – Very High Resolution, MR – Medium Resolution, CNN – Convolutional Neural Network.

3 Results

The total area of disturbed forest patches amounted to nearly 21.73 km^2, which is equivalent to 1.82% of the total forest cover. Almost 70% of the disturbed patches were concentrated within dark coniferous forests, while > 27% occurred in mixedwood forests, and approximately 1% in birch forests. Other forest types accounted for < 2% of the disturbed areas. Large patches over 1 hectare constituted 38.5% of windthrows. Intermediate-sized canopy gaps (0.01–1 ha) represented 37.5%, and small gaps (less than 0.01 ha) comprised 26.7% of the total disturbed area (Fig. 7). Most trees were uprooted rather than broken, as evidenced by visible root pits in VHR satellite images and confirmed by our ground observations (Fig. 8).

Forests on slopes with aspect from 10 to 170° demonstrated a higher vulnerability to disturbance, whereas western slopes exhibited a lower proportion of damaged forest (Fig. 9a). The distribution of windthrow occurrences concerning elevation and slope steepness indicates that forests at altitudes between 10 and 150 m above sea level on less steep slopes experienced more pronounced disturbances. In contrast, forests situated above 150 m in elevation and on slopes steeper than approximately 15° showed a lower susceptibility to disturbances (Fig. 9b and 9c). Forests with a canopy closure below roughly 70% were less susceptible to windthrow compared to those with denser canopies (Fig. 9d). Terrain curvature did not present any significant

https://doi.org/10.5194/nhess-2024-217
Preprint. Discussion started: 15 January 2025

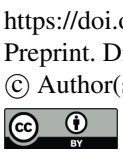

Natural Hazards and Earth System Sciences
Discussions

influence on the severity of disturbance (Fig. 9e). Landform classes, specifically 'flat', 'footslope', 'shoulder', 'peak', 'ridge', and 'pit', exhibited a higher proportion of windthrows (Fig. 9f).

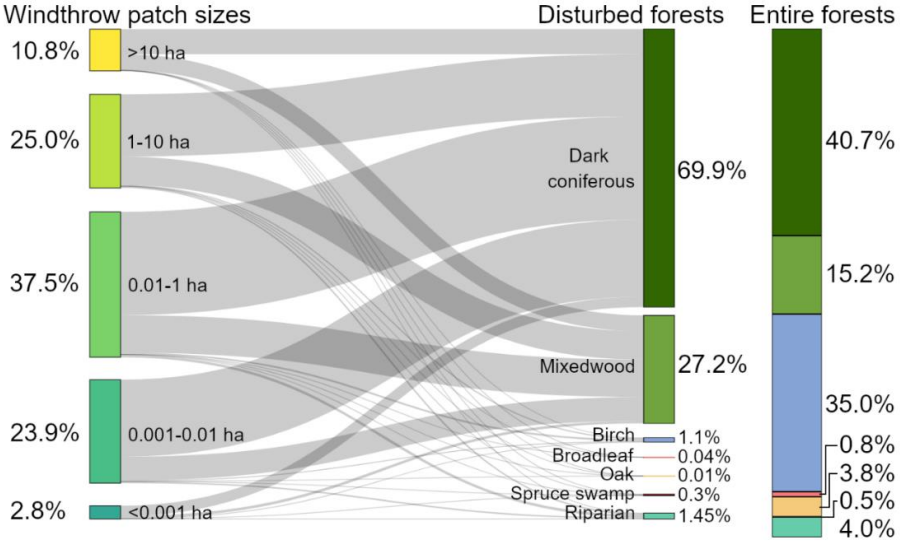

Figure 7: Proportional distribution of windthrow disturbances among forest types compared to total forest composition.

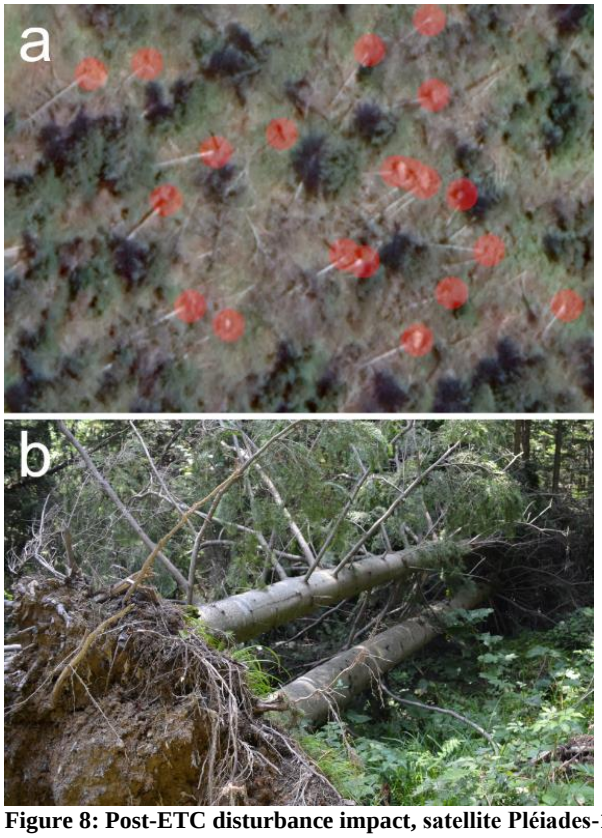

225 **Figure 8: Post-ETC disturbance impact, satellite Pléiades-1(a) and ground survey (b) images of uprooted trees.**

https://doi.org/10.5194/nhess-2024-217
Preprint. Discussion started: 15 January 2025

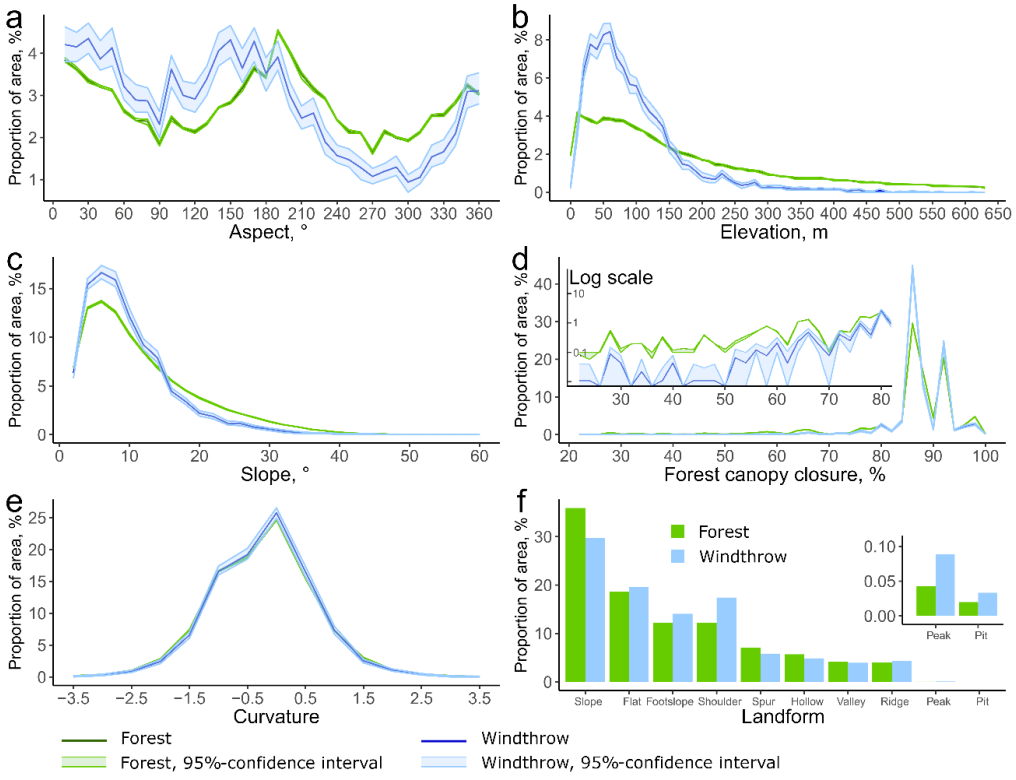

Figure 9: Comparative distribution of the proportion of damaged forest areas and entire forest cover across different environmental predictors in Kunashir Island. Non-overlapping 95% confidence intervals indicate a statistically significant difference.

The RF analysis identified 'elevation' as the most influential predictor for the risk of damage, accounting for over 45% of the feature importance. In contrast, 'curvature' and 'landform' exerted the least impact on the outcome of the RF model (Fig. 10). The optimal combination of predictors, which achieved the highest BA score, includes 'aspect,' 'slope,' 'elevation,' 'canopy closure,' 'landform type,' and 'vegetation type'. A list of the top 99 predictor combinations, with BA scores ranging from 0.72 to 0.55 (Table in Supplementary 3). However, we observed a complex interplay among elevation, canopy closure, slope steepness, and forest types (Fig. 11), indicating that these factors do not independently determine windthrow vulnerability.

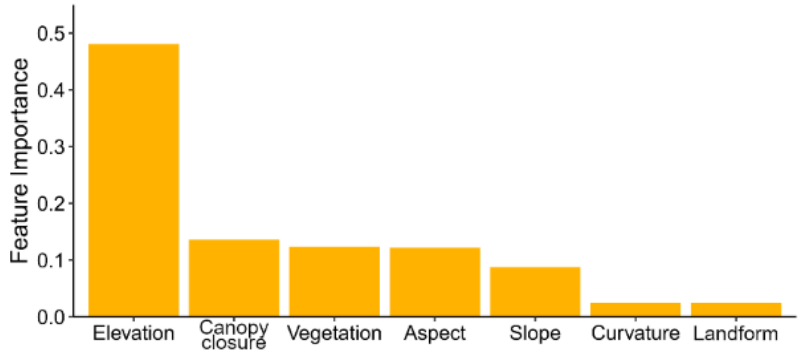

Figure 10: Feature importance scores for the RF results.

https://doi.org/10.5194/nhess-2024-217
Preprint. Discussion started: 15 January 2025

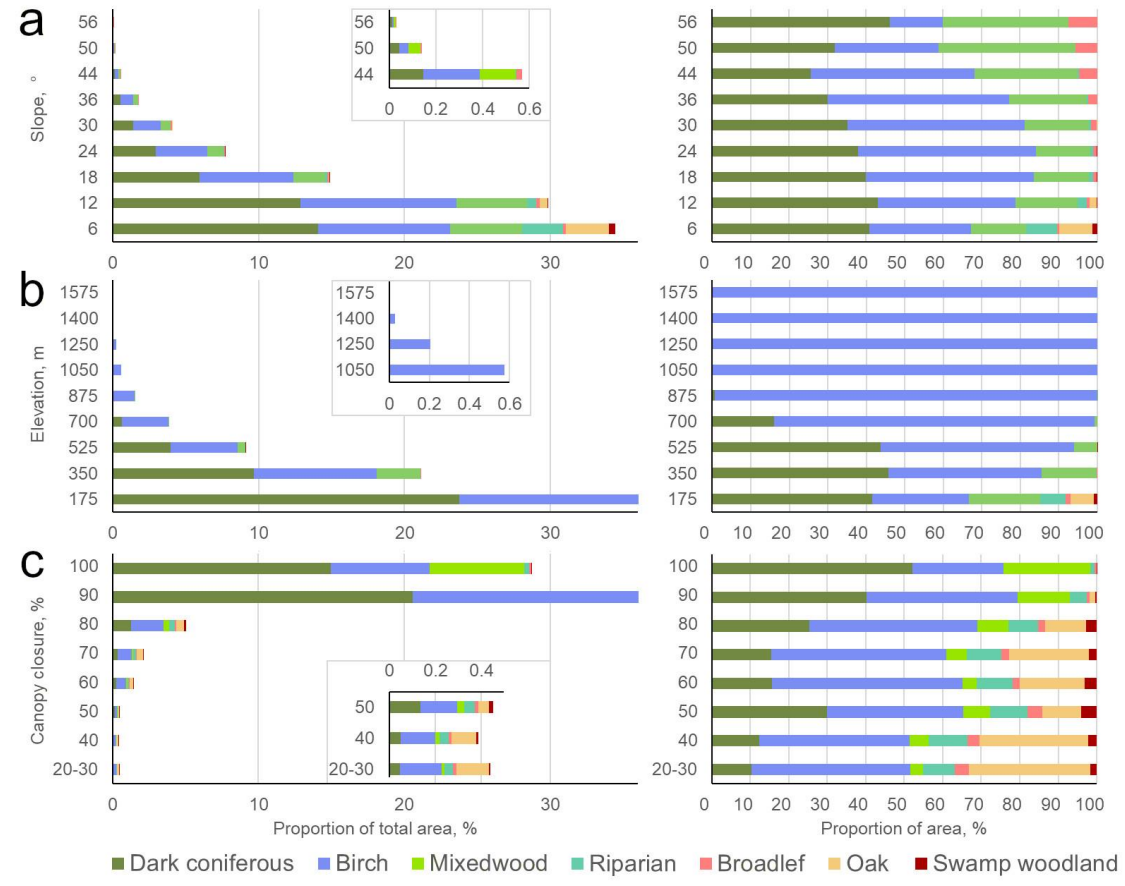

Figure 11: Distribution of different forest types across slope steepness (a), elevation (b), and canopy closure (c).

4 Discussion

Using CNN and machine learning techniques, we identified the elevation gradient as a pivotal factor in the disturbance risk models, primarily due to its connection with varying forest types. The elevation gradient reflects a complex ecological pattern representing the suite of ecological and climatic factors that collectively influence forest vulnerability to disturbance (Černý et al., 2022). Our analysis revealed a pronounced susceptibility to damage in dark coniferous and mixedwood forests dominated by spruces and firs, which are predominantly situated in low-elevation areas and characterized by high canopy closure, making them more vulnerable to the ETC event. Conversely, open canopy forests, particularly those with oak and birches, exhibited lower disturbance rates and demonstrated resistance to the ETC event. Naturally developed open canopy forest stands are adapted to open-grown conditions, contributing to their higher resistance to windthrow (Taylor et al., 2019). Open-canopy forests resulting from logging or sparse plantations face a higher risk of windthrow (Suvanto et al., 2016; Valinger and Fridman, 2011).

https://doi.org/10.5194/nhess-2024-217
Preprint. Discussion started: 15 January 2025


Natural Hazards and Earth System Sciences Discussions

Our results align with the established understanding that coniferous evergreen trees are more susceptible to winter storm damage compared to broadleaf trees with leafless canopies (Zeppenfeld et al., 2023). While spruces and firs show a higher risk for storm and snow damage, broadleaf hardwoods demonstrate greater resistance (Barrere et al., 2023). In previous studies, we also reported a higher risk of windthrow severity for natural dark coniferous forests compared to broadleaf forests (Černý et al., 2022; Korznikov et al., 2023, 2022). The tree species from the mountain areas of Northeast Asia adapted to intensive snowfalls (Krestov, 2003; Nakamura and Krestov, 2005; Shamshin, 1999). The greater resistance of mountain birch forests to disturbance can be attributed to structural characteristics or adaptations that stone birch trees have evolved to withstand high wind speeds and heavy snowfall (Gansert, 2002; Krestov, 2003; Shamshin, 1999). The leafless crowns of stone birch do not accumulate more than 1–1.2 cm of snow, which is insufficient to cause significant crown damage (Suzuki et al., 2008). A 1 cm layer of snow in the humid winter conditions, typical of Northern Japan or the Southern Kuril Islands, adds an equivalent weight of 2 kg m^{-2}. Thus, a snow layer of 6–7 cm on tree crowns exceeds the crown weights for firs and spruces, and external loading has a more substantial effect on tree stability than self-weight does (Nishimura, 2005). Therefore, the estimated accumulation of 8 cm of wet snow during the ETC event was sufficient to cause damage and massive disturbances, especially in combination with high-velocity wind gusts.

Our findings indicate that mixedwood forests exhibited a high sensitivity to ETC disturbances. In contrast, (Morimoto et al., 2019) observed that Sakhalin fir artificial stands in Northern Japan consistently experienced higher windthrow ratios than natural mixedwood forests. An admixture of 25–30% deciduous trees in spruce-dominated stands could reduce the probability of winter storm damage by approximately 50% (Valinger and Fridman, 2011). During the ETC event in Kunashir, disturbances within mixedwood forests predominantly occurred in patches of coniferous trees, while patches dominated by broadleaf trees showed greater resistance. Therefore, it is critical to recognize that the significant levels of disturbance in Kunashir's mixedwood forests are primarily due to damage to conifers. In essence, the ETC has decreased the proportion of coniferous trees in the mixedwood forests and the entire forest cover.

The distribution of forest disturbance patches across the landscape is complex and seems to be linked to snow accumulation as well as wind exposure. Our findings highlight that individual predictors are not universal factors of windthrow risk and that the relevance depends on the specific context of the landscape and vegetation, as well as the wind and precipitation dynamic of the weather phenomenon causing the disturbance. The potential contribution of individual factors may be reduced when creating more sophisticated models that consider multiple predictors, due to their intercorrelation. Forest damage risk assessment relies on elucidating the interactions among predictors and understanding how they influence disturbance severity when interacting. Based on our experience, it is often impossible to acquire such comprehensive insight by working exclusively with remote sensing data. Ground-based research and understanding of the landscape context and forest cover features remain extremely important both for the selection of environmental predictors explaining the hazard of wind disturbance and for the correct interpretation of the disturbance risk model.

https://doi.org/10.5194/nhess-2024-217
Preprint. Discussion started: 15 January 2025


Natural Hazards and Earth System Sciences Discussions

5 Conclusions

We developed and implemented a robust analytical framework to analyze spatial patterns of forest disturbance caused by a severe weather event. Using the U-Net CNN, we precisely identified windthrow patches totalling 21.73 km² (1.82% of the forested area) affected by the disturbance. Our retrospective risk assessment, employing the RF algorithm and various environmental predictors, enhanced our understanding of past disturbances and assessed potential future risks under evolving disturbance regimes. We found that the primary hazard of forest damage arose from wet snow accumulation on evergreen coniferous trees, significantly increasing their vulnerability. Approximately 70% of the windthrow occurred in dark coniferous spruce and fir forests. In contrast, broadleaf deciduous trees, particularly subalpine stone birch at higher elevations, showed lower susceptibility to disturbance. The optimal windthrow risk model included topographic factors of aspect, elevation, slope steepness, and landform class, along with forest canopy closure and forest type. Our approach can assess post-ETC forest disturbances, offering critical insights into forest loss and recurrence risks due to increasing extreme weather events from global warming. This is essential for sustainable forestry and effective management strategies.

Code and data availability

The data is available upon request to the correspondence author. The code is available in Supplementary 1 and 2.

Author contributions

KK: conceptualization, writing (original draft), formal analysis, and visualization. DK: data curation, formal analysis, software; writing (review and editing). JD: writing (review and editing). JA: funding acquisition, writing (review and editing).

Competing interests

The contact author has declared that none of the authors has any competing interests.

Disclaimer

Publisher's note: Copernicus Publications remains neutral with regard to jurisdictional claims made in the text, published maps, institutional affiliations, or any other geographical representation in this paper. While Copernicus Publications makes every effort to include appropriate place names, the final responsibility lies with the authors.

Financial support

This research has been supported by the research grant 23-05272S of the Czech Science Foundation, the long-term research development project No. RVO 67985939 of the Czech Academy of Sciences, and and scientific framework of the Botanical Garden-Institute FEB RAS (FWFR-2022-0008) No. 122040800089-2.

Acknowledgements

We thank all our colleagues for their participation and assistance in field research on Kunashir Island in 2019 and 2021.

https://doi.org/10.5194/nhess-2024-217
Preprint. Discussion started: 15 January 2025

References

Altman, J., Fibich, P., Trotsiuk, V.,and Altmanova, N.: Global pattern of forest disturbances and its shift under climate change. Science of The Total Environment 915:170117. https://doi.org/10.1016/j.scitotenv.2024.170117, 2024.

Anderson-Teixeira, K.J., Herrmann, V., Morgan RB, et al (2021) Carbon cycling in mature and regrowth forests globally. Environ Res Lett 16:053009. https://doi.org/10.1088/1748-9326/abed01

Barrere J, Reineking B, Cordonnier T, et al (2023) Functional traits and climate drive interspecific differences in disturbance-induced tree mortality. Global Change Biology 29:2836–2851. https://doi.org/10.1111/gcb.16630

Černý T, Doležal J, Petřík P, et al (2022) Tropical Cyclone Disturbances Induce Contrasting Impacts on Forest Structure, Plant Composition, and Soil Properties in Temperate Broadleaf and Coniferous Forests. Forests 13:1033. https://doi.org/10.3390/f13071033

Chen N, Tsendbazar N-E, Hamunyela E, et al (2021) Sub-annual tropical forest disturbance monitoring using harmonized Landsat and Sentinel-2 data. International Journal of Applied Earth Observation and Geoinformation 102:102386. https://doi.org/10.1016/j.jag.2021.102386

Curtis PG, Slay CM, Harris NL, et al (2018) Classifying drivers of global forest loss. Science 361:1108–1111. https://doi.org/10.1126/science.aau3445

Everham EM, Brokaw NVL (1996) Forest damage and recovery from catastrophic wind. Bot Rev 62:113–185. https://doi.org/10.1007/BF02857920

Foster DR (1988) Species and Stand Response to Catastrophic Wind in Central New England, U.S.A. Journal of Ecology 76:135–151. https://doi.org/10.2307/2260458

Gansert D (2002) Betula ermanii, a Dominant Subalpine and Subarctic Treeline Tree Species in Japan: Ecological Traits of Deciduous Tree Life in Winter. Arctic, Antarctic, and Alpine Research 34:57–64. https://doi.org/10.1080/15230430.2002.12003469

Hansen MC, Potapov PV, Moore R, et al (2013) High-Resolution Global Maps of 21st-Century Forest Cover Change. Science 342:850–853. https://doi.org/10.1126/science.1244693

Jasiewicz J, Stepinski TF (2013) Geomorphons — a pattern recognition approach to classification and mapping of landforms. Geomorphology 182:147–156. https://doi.org/10.1016/j.geomorph.2012.11.005

Jin S, Sader SA (2005) MODIS time-series imagery for forest disturbance detection and quantification of patch size effects. Remote Sensing of Environment 99:462–470. https://doi.org/10.1016/j.rse.2005.09.017

Kattenborn T, Leitloff J, Schiefer F, Hinz S (2021) Review on Convolutional Neural Networks (CNN) in vegetation remote sensing. ISPRS Journal of Photogrammetry and Remote Sensing 173:24–49. https://doi.org/10.1016/j.isprsjprs.2020.12.010

Kislov DE, Korznikov KA (2020) Automatic Windthrow Detection Using Very-High-Resolution Satellite Imagery and Deep Learning. Remote Sensing 12:1145. https://doi.org/10.3390/rs12071145

https://doi.org/10.5194/nhess-2024-217
Preprint. Discussion started: 15 January 2025

Kislov DE, Korznikov KA, Altman J, et al (2021) Extending deep learning approaches for forest disturbance segmentation on very high-resolution satellite images. Remote Sensing in Ecology and Conservation 7:355–368. https://doi.org/10.1002/rse2.194

Korznikov K, Kislov D, Doležal J, et al (2022) Tropical cyclones moving into boreal forests: Relationships between disturbance areas and environmental drivers. Science of The Total Environment 844:156931. https://doi.org/10.1016/j.scitotenv.2022.156931

Korznikov K, Petrenko T, Kislov D, et al (2023) Predicting Spruce Taiga Distribution in Northeast Asia Using Species Distribution Models: Glacial Refugia, Mid-Holocene Expansion and Future Predictions for Global Warming. Forests 14:219. https://doi.org/10.3390/f14020219

Korznikov KA, Altman J, Belyaeva NG, et al (2024) Boreal to temperate forests transition within Kunashir Island (the Kuril Archipelago): Insights from the novel vegetation map. Botanica Pacifica 13(1):37–43. https://doi.org/10.17581/bp.2024.13109

Krestov PV (2003) Forest Vegetation of Easternmost Russia (Russian Far East). In: Kolbek J, Šrůtek M, Box EO (eds) Forest Vegetation of Northeast Asia. Springer Netherlands, Dordrecht, pp 93–180

Little AS, Priestley MDK, Catto JL (2023) Future increased risk from extratropical windstorms in northern Europe. Nat Commun 14:4434. https://doi.org/10.1038/s41467-023-40102-6

Liu S, Bond-Lamberty B, Hicke JA, et al (2011) Simulating the impacts of disturbances on forest carbon cycling in North America: Processes, data, models, and challenges. Journal of Geophysical Research: Biogeosciences 116:. https://doi.org/10.1029/2010JG001585

Mitchell SJ (2013) Wind as a natural disturbance agent in forests: a synthesis. Forestry: An International Journal of Forest Research 86:147–157. https://doi.org/10.1093/forestry/cps058

Montagné-Huck C, Brunette M (2018) Economic analysis of natural forest disturbances: A century of research. Journal of Forest Economics 32:42–71. https://doi.org/10.1016/j.jfe.2018.03.002

Morimoto J, Nakagawa K, Takano KT, et al (2019) Comparison of vulnerability to catastrophic wind between Abies plantation forests and natural mixed forests in northern Japan. Forestry: An International Journal of Forest Research 92:436–443. https://doi.org/10.1093/forestry/cpy045

Nakamura, Yu., Krestov, P.V., 2005. Coniferous forests of the temperate zone of Asia, in: Andersson, F.A. (Ed.), Coniferous Forests of the Temperate Zone of Asia, Ecosystems of the World. Elsevier.

Nishimura TB (2005) Tree characteristics related to stem breakage of Picea glehnii and Abies sachalinensis. Forest Ecology and Management 215:295–306. https://doi.org/10.1016/j.foreco.2005.05.018

Pedregosa F, Varoquaux G, Gramfort A, et al (2011) Scikit-learn: Machine Learning in Python. MACHINE LEARNING IN PYTHON

Pojar J, Klinka K, Meidinger DV (1987) Biogeoclimatic ecosystem classification in British Columbia. Forest Ecology and Management 22:119–154. https://doi.org/10.1016/0378-1127(87)90100-9

https://doi.org/10.5194/nhess-2024-217
Preprint. Discussion started: 15 January 2025

Priestley MDK, Catto JL (2022) Future changes in the extratropical storm tracks and cyclone intensity, wind speed, and structure. Weather and Climate Dynamics 3:337–360. https://doi.org/10.5194/wcd-3-337-2022

Pugh TAM, Arneth A, Kautz M, et al (2019) Important role of forest disturbances in the global biomass turnover and carbon sinks. Nat Geosci 12:730–735. https://doi.org/10.1038/s41561-019-0427-2

Roos A (2023) Forest damage and forest supply chains: a literature review and reflections. International Journal of Forest Engineering 0:1–10. https://doi.org/10.1080/14942119.2023.2240607

Sánchez JJ, Marcos-Martinez R, Srivastava L, Soonsawad N (2021) Valuing the impacts of forest disturbances on ecosystem services: An examination of recreation and climate regulation services in U.S. national forests. Trees, Forests and People 5:100123. https://doi.org/10.1016/j.tfp.2021.100123

Seidl R, Rammer W (2017) Climate change amplifies the interactions between wind and bark beetle disturbances in forest landscapes. Landscape Ecol 32:1485–1498. https://doi.org/10.1007/s10980-016-0396-4

Seidl R, Thom D, Kautz M, et al (2017) Forest disturbances under climate change. Nature Clim Change 7:395–402. https://doi.org/10.1038/nclimate3303

Seidl R, Turner MG (2022) Post-disturbance reorganization of forest ecosystems in a changing world. Proc Natl Acad Sci USA 119:e2202190119. https://doi.org/10.1073/pnas.2202190119

Shamshin VA (1999) The stone birch forests of Kamchatka: biology, ecology and stand structure. GEOS, Moscow

Suvanto S, Henttonen HM, Nöjd P, Mäkinen H (2016) Forest susceptibility to storm damage is affected by similar factors regardless of storm type: Comparison of thunder storms and autumn extra-tropical cyclones in Finland. Forest Ecology and Management 381:17–28. https://doi.org/10.1016/j.foreco.2016.09.005

Suvanto S, Peltoniemi M, Tuominen S, et al (2019) High-resolution mapping of forest vulnerability to wind for disturbance-aware forestry. Forest Ecology and Management 453:117619. https://doi.org/10.1016/j.foreco.2019.117619

Suzuki K, Kodama Y, Yamazaki T, et al (2008) Snow accumulation on evergreen needle-leaved and deciduous broad-leaved trees. Boreal Environment Research 13:403–416

Taylor AR, Dracup E, MacLean DA, et al (2019) Forest structure more important than topography in determining windthrow during Hurricane Juan in Canada's Acadian Forest. Forest Ecology and Management 434:255–263. https://doi.org/10.1016/j.foreco.2018.12.026

Thom D, Seidl R (2016) Natural disturbance impacts on ecosystem services and biodiversity in temperate and boreal forests. Biological Reviews 91:760–781. https://doi.org/10.1111/brv.12193

Tyukavina A, Potapov P, Hansen MC, et al (2022) Global Trends of Forest Loss Due to Fire From 2001 to 2019. Front Remote Sens 3:825190. https://doi.org/10.3389/frsen.2022.825190

Valinger E, Fridman J (2011) Factors affecting the probability of windthrow at stand level as a result of Gudrun winter storm in southern Sweden. Forest Ecology and Management 262:398–403. https://doi.org/10.1016/j.foreco.2011.04.004

Zeppenfeld T, Jung C, Schindler D, et al (2023) Winter storm risk assessment in forests with high resolution gust speed data. Eur J Forest Res 142:1045–1058. https://doi.org/10.1007/s10342-023-01575-8

415 Zhang Y, Ling F, Wang X, et al (2021) Tracking small-scale tropical forest disturbances: Fusing the Landsat and Sentinel-2 data record. Remote Sensing of Environment 261:112470. https://doi.org/10.1016/j.rse.2021.112470

Abrams, M., Crippen, R., and Fujisada, H.: ASTER Global Digital Elevation Model (GDEM) and ASTER Global Water Body Dataset (ASTWBD), Remote Sensing, 12, 1156, https://doi.org/10.3390/rs12071156, 2020.

420 Altman, J., Fibich, P., Trotsiuk, V., and Altmanova, N.: Global pattern of forest disturbances and its shift under climate change, Science of The Total Environment, 915, 170117, https://doi.org/10.1016/j.scitotenv.2024.170117, 2024.

Anderson-Teixeira, K. J., Herrmann, V., Morgan, R. B., Bond-Lamberty, B., Cook-Patton, S. C., Ferson, A. E., Muller-Landau, H. C., and Wang, M. M. H.: Carbon cycling in mature and regrowth forests globally, Environ. Res. Lett., 16, 053009, https://doi.org/10.1088/1748-9326/abed01, 2021.

425 ArcMap documentation. https://desktop.arcgis.com/en/arcmap/latest/tools/3d-analyst-toolbox/an-overview-of-the-raster-surface-toolset.htm, 2024

Barrere, J., Reineking, B., Cordonnier, T., Kulha, N., Honkaniemi, J., Peltoniemi, M., Korhonen, K. T., Ruiz-Benito, P., Zavala, M. A., and Kunstler, G.: Functional traits and climate drive interspecific differences in disturbance-induced tree mortality, Global Change Biology, 29, 2836–2851, https://doi.org/10.1111/gcb.16630, 2023.

430 Černý, T., Doležal, J., Petřík, P., Šrůtek, M., Song, J.-S., and Altman, J.: Tropical Cyclone Disturbances Induce Contrasting Impacts on Forest Structure, Plant Composition, and Soil Properties in Temperate Broadleaf and Coniferous Forests, Forests, 13, 1033, https://doi.org/10.3390/f13071033, 2022.

Chen, N., Tsendbazar, N.-E., Hamunyela, E., Verbesselt, J., and Herold, M.: Sub-annual tropical forest disturbance monitoring using harmonized Landsat and Sentinel-2 data, International Journal of Applied Earth Observation and Geoinformation, 102,

435 102386, https://doi.org/10.1016/j.jag.2021.102386, 2021.

Curtis, P. G., Slay, C. M., Harris, N. L., Tyukavina, A., and Hansen, M. C.: Classifying drivers of global forest loss, Science, 361, 1108–1111, https://doi.org/10.1126/science.aau3445, 2018.

Everham, E. M. and Brokaw, N. V. L.: Forest damage and recovery from catastrophic wind, Bot. Rev, 62, 113–185, https://doi.org/10.1007/BF02857920, 1996.

440 Foster, D. R.: Species and Stand Response to Catastrophic Wind in Central New England, U.S.A., Journal of Ecology, 76, 135–151, https://doi.org/10.2307/2260458, 1988.

Gansert, D.: Betula ermanii, a Dominant Subalpine and Subarctic Treeline Tree Species in Japan: Ecological Traits of Deciduous Tree Life in Winter, Arctic, Antarctic, and Alpine Research, 34, 57–64, https://doi.org/10.1080/15230430.2002.12003469, 2002.

445 Hansen, M. C., Potapov, P. V., Moore, R., Hancher, M., Turubanova, S. A., Tyukavina, A., Thau, D., Stehman, S. V., Goetz, S. J., Loveland, T. R., Kommareddy, A., Egorov, A., Chini, L., Justice, C. O., and Townshend, J. R. G.: High-Resolution Global Maps of 21st-Century Forest Cover Change, Science, 342, 850–853, https://doi.org/10.1126/science.1244693, 2013.

https://doi.org/10.5194/nhess-2024-217
Preprint. Discussion started: 15 January 2025

Jasiewicz, J. and Stepinski, T. F.: Geomorphons — a pattern recognition approach to classification and mapping of landforms, Geomorphology, 182, 147–156, https://doi.org/10.1016/j.geomorph.2012.11.005, 2013.

Jin, S. and Sader, S. A.: MODIS time-series imagery for forest disturbance detection and quantification of patch size effects, Remote Sensing of Environment, 99, 462–470, https://doi.org/10.1016/j.rse.2005.09.017, 2005.

Kattenborn, T., Leitloff, J., Schiefer, F., and Hinz, S.: Review on Convolutional Neural Networks (CNN) in vegetation remote sensing, ISPRS Journal of Photogrammetry and Remote Sensing, 173, 24–49, https://doi.org/10.1016/j.isprsjprs.2020.12.010, 2021.

Kislov, D. E. and Korznikov, K. A.: Automatic Windthrow Detection Using Very-High-Resolution Satellite Imagery and Deep Learning, Remote Sensing, 12, 1145, https://doi.org/10.3390/rs12071145, 2020.

Kislov, D. E., Korznikov, K. A., Altman, J., Vozmishcheva, A. S., and Krestov, P. V.: Extending deep learning approaches for forest disturbance segmentation on very high-resolution satellite images, Remote Sensing in Ecology and Conservation, 7, 355–368, https://doi.org/10.1002/rse2.194, 2021.

Korznikov, K., Kislov, D., Doležal, J., Petrenko, T., and Altman, J.: Tropical cyclones moving into boreal forests: Relationships between disturbance areas and environmental drivers, Science of The Total Environment, 844, 156931, https://doi.org/10.1016/j.scitotenv.2022.156931, 2022.

Korznikov, K., Petrenko, T., Kislov, D., Krestov, P., and Doležal, J.: Predicting Spruce Taiga Distribution in Northeast Asia Using Species Distribution Models: Glacial Refugia, Mid-Holocene Expansion and Future Predictions for Global Warming, Forests, 14, 219, https://doi.org/10.3390/f14020219, 2023.

Korznikov, K. A., Altman, J., Institute of Botany CAS, Belyaeva, N. G., Institute of Geography RAS, Dzizyurova, V. D., Botanical garden-institute FEB RAS, Lomonosov Moscow State University, Kislov, D. E., Botanical garden-institute FEB RAS, Linnik, E. V., Kurilsky Nature Reserve, Petrenko, T. Ya., and Botanical garden-institute FEB RAS: Boreal to temperate forests transition within Kunashir Island (the Kuril Archipelago): Insights from the novel vegetation map, Bot Pac, https://doi.org/10.17581/bp.2024.13109, 2024.

Krestov, P. V.: Forest Vegetation of Easternmost Russia (Russian Far East), in: Forest Vegetation of Northeast Asia, edited by: Kolbek, J., Šrůtek, M., and Box, E. O., Springer Netherlands, Dordrecht, 93–180, https://doi.org/10.1007/978-94-017-0143-3_5, 2003.

Little, A. S., Priestley, M. D. K., and Catto, J. L.: Future increased risk from extratropical windstorms in northern Europe, Nat Commun, 14, 4434, https://doi.org/10.1038/s41467-023-40102-6, 2023.

Liu, S., Bond-Lamberty, B., Hicke, J. A., Vargas, R., Zhao, S., Chen, J., Edburg, S. L., Hu, Y., Liu, J., McGuire, A. D., Xiao, J., Keane, R., Yuan, W., Tang, J., Luo, Y., Potter, C., and Oeding, J.: Simulating the impacts of disturbances on forest carbon cycling in North America: Processes, data, models, and challenges, Journal of Geophysical Research: Biogeosciences, 116, https://doi.org/10.1029/2010JG001585, 2011.

Mitchell, S. J.: Wind as a natural disturbance agent in forests: a synthesis, Forestry: An International Journal of Forest Research, 86, 147–157, https://doi.org/10.1093/forestry/cps058, 2013.

https://doi.org/10.5194/nhess-2024-217
Preprint. Discussion started: 15 January 2025

Morimoto, J., Nakagawa, K., Takano, K. T., Aiba, M., Oguro, M., Furukawa, Y., Mishima, Y., Ogawa, K., Ito, R., Takemi, T., Nakamura, F., and Peterson, C. J.: Comparison of vulnerability to catastrophic wind between Abies plantation forests and natural mixed forests in northern Japan, Forestry: An International Journal of Forest Research, 92, 436–443, https://doi.org/10.1093/forestry/cpy045, 2019.

Nakamura, Yu. and Krestov, P. V.: Coniferous forests of the temperate zone of Asia, in: Coniferous forests of the temperate zone of Asia, vol. 6, edited by: Andersson, F. A., Elsevier, 2005.

Nishimura, T. B.: Tree characteristics related to stem breakage of Picea glehnii and Abies sachalinensis, Forest Ecology and Management, 215, 295–306, https://doi.org/10.1016/j.foreco.2005.05.018, 2005.

Pedregosa, F., Varoquaux, G., Gramfort, A., Michel, V., Thirion, B., Grisel, O., Blondel, M., Prettenhofer, P., Weiss, R., Dubourg, V., Vanderplas, J., Passos, A., and Cournapeau, D.: Scikit-learn: Machine Learning in Python, MACHINE LEARNING IN PYTHON, 2011.

Pojar, J., Klinka, K., and Meidinger, D. V.: Biogeoclimatic ecosystem classification in British Columbia, Forest Ecology and Management, 22, 119–154, https://doi.org/10.1016/0378-1127(87)90100-9, 1987.

Priestley, M. D. K. and Catto, J. L.: Future changes in the extratropical storm tracks and cyclone intensity, wind speed, and structure, Weather and Climate Dynamics, 3, 337–360, https://doi.org/10.5194/wcd-3-337-2022, 2022.

Pugh, T. A. M., Arneth, A., Kautz, M., Poulter, B., and Smith, B.: Important role of forest disturbances in the global biomass turnover and carbon sinks, Nat Geosci, 12, 730–735, https://doi.org/10.1038/s41561-019-0427-2, 2019.

Roos, A.: Forest damage and forest supply chains: a literature review and reflections, International Journal of Forest Engineering, 0, 1–10, https://doi.org/10.1080/14942119.2023.2240607, 2023.

Seidl, R. and Rammer, W.: Climate change amplifies the interactions between wind and bark beetle disturbances in forest landscapes, Landscape Ecol, 32, 1485–1498, https://doi.org/10.1007/s10980-016-0396-4, 2017.

Seidl, R. and Turner, M. G.: Post-disturbance reorganization of forest ecosystems in a changing world, Proc. Natl. Acad. Sci. U.S.A., 119, e2202190119, https://doi.org/10.1073/pnas.2202190119, 2022.

Seidl, R., Thom, D., Kautz, M., Martin-Benito, D., Peltoniemi, M., Vacchiano, G., Wild, J., Ascoli, D., Petr, M., Honkaniemi, J., Lexer, M. J., Trotsiuk, V., Mairota, P., Svoboda, M., Fabrika, M., Nagel, T. A., and Reyer, C. P. O.: Forest disturbances under climate change, Nature Clim Change, 7, 395–402, https://doi.org/10.1038/nclimate3303, 2017.

Shamshin, V. A.: The stone birch forests of Kamchatka: biology, ecology and stand structure., GEOS, Moscow, 170 pp., 1999.

Suvanto, S., Henttonen, H. M., Nöjd, P., and Mäkinen, H.: Forest susceptibility to storm damage is affected by similar factors regardless of storm type: Comparison of thunder storms and autumn extra-tropical cyclones in Finland, Forest Ecology and Management, 381, 17–28, https://doi.org/10.1016/j.foreco.2016.09.005, 2016.

Suvanto, S., Peltoniemi, M., Tuominen, S., Strandström, M., and Lehtonen, A.: High-resolution mapping of forest vulnerability to wind for disturbance-aware forestry, Forest Ecology and Management, 453, 117619, https://doi.org/10.1016/j.foreco.2019.117619, 2019.

https://doi.org/10.5194/nhess-2024-217
Preprint. Discussion started: 15 January 2025

515 Suzuki, K., Kodama, Y., Yamazaki, T., Kosugi, K., and Nakai, Y.: Snow accumulation on evergreen needle-leaved and deciduous broad-leaved trees, Boreal Environment Research, 13, 403–416, 2008.

Taylor, A. R., Dracup, E., MacLean, D. A., Boulanger, Y., and Endicott, S.: Forest structure more important than topography in determining windthrow during Hurricane Juan in Canada's Acadian Forest, Forest Ecology and Management, 434, 255–263, https://doi.org/10.1016/j.foreco.2018.12.026, 2019.

520 Thom, D. and Seidl, R.: Natural disturbance impacts on ecosystem services and biodiversity in temperate and boreal forests, Biological Reviews, 91, 760–781, https://doi.org/10.1111/brv.12193, 2016.

Tyukavina, A., Potapov, P., Hansen, M. C., Pickens, A. H., Stehman, S. V., Turubanova, S., Parker, D., Zalles, V., Lima, A., Kommareddy, I., Song, X.-P., Wang, L., and Harris, N.: Global Trends of Forest Loss Due to Fire From 2001 to 2019, Front. Remote Sens., 3, 825190, https://doi.org/10.3389/frsen.2022.825190, 2022.

525 Valinger, E. and Fridman, J.: Factors affecting the probability of windthrow at stand level as a result of Gudrun winter storm in southern Sweden, Forest Ecology and Management, 262, 398–403, https://doi.org/10.1016/j.foreco.2011.04.004, 2011.

Zeppenfeld, T., Jung, C., Schindler, D., Sennhenn-Reulen, H., Ipsen, M. J., and Schmidt, M.: Winter storm risk assessment in forests with high resolution gust speed data, Eur J Forest Res, 142, 1045–1058, https://doi.org/10.1007/s10342-023-01575-8, 2023.

530 Zhang, Y., Ling, F., Wang, X., Foody, G. M., Boyd, D. S., Li, X., Du, Y., and Atkinson, P. M.: Tracking small-scale tropical forest disturbances: Fusing the Landsat and Sentinel-2 data record, Remote Sensing of Environment, 261, 112470, https://doi.org/10.1016/j.rse.2021.112470, 2021.